

Multifunctional rare earth or bismuth oxide materials for catalytic or electrical applications

J.R. Gavarri^{1,a}, L. Bourja^{1,2}, B. Bakiz^{1,2}, F. Guinneton¹, S. Villain¹, M. Arab¹, A. Benlhachemi² and M. Ezahri²

¹ *Institut Matériaux Microélectronique et Nanosciences de Provence, IM2NP, UMR CNRS 7334, Université du Sud Toulon-Var, BP. 20132, 83957 La Garde Cedex, France*

² *Laboratoire Matériaux et Environnement LME, Faculté des Sciences, Université Ibn Zohr, BP. 8106, Cité Dakhla, Agadir, Maroc*

Abstract. We present a review on catalytic or electrical properties of materials based on rare earth (RE) oxides (CeO_2 , La_2O_3 , Lu_2O_3) or bismuth based composite systems CeO_2 - Bi_2O_3 , susceptible to be integrated into catalytic microsystems or gas sensors. The polycrystalline solids can be used as catalysts allowing conversion of CO or CH_4 traces in air-gas flows. Fourier Transform infrared spectroscopy is used to determine the conversion rate of CO or CH_4 into CO_2 through the variations versus time and temperature of vibrational band intensities. The time dependent reactivities are interpreted in terms of an adapted Avrami model. In these catalytic analyses the nature of surfaces of polycrystalline solids seems to play a prominent role in catalytic efficiency. Electrical impedance spectroscopy allows analyzing the variation of conductivity of the system CeO_2 - Bi_2O_3 . In this system, the specific high ionic conduction of a Bi_2O_3 tetragonal phase might be linked to the high catalytic activity.

1. INTRODUCTION

In the case of RE oxide [1,2] and CeO_2 - Bi_2O_3 materials [3,4], infrared spectroscopy as a function of time (t) and temperature (T) has been used to determine the catalytic oxidation rates of CH_4 or CO into CO_2 . In the case of bismuth based system $[(1-x)\text{CeO}_2 - (x/2)\text{Bi}_2\text{O}_3]$ with $0 < x < 1$, electrical impedance spectroscopy (EIS) has been used to determine the conductivities as a function of bismuth fraction (x) and temperature (T). We try to give a general interpretation of the origin of abnormal catalytic effects in the case of methane or carbon monoxide oxidation in air, as these gases are in contact with the above RE or Bi based solids at high temperature. High temperature ionic conduction coupled to complex surface modifications of these solids might be at the origin of strongly different catalytic effects.

2. CATALYTIC APPLICATIONS

2.1. Rare earth oxides for catalytic applications

The polycrystalline RE oxides (CeO_2 , La_2O_3 , Lu_2O_3) have been subjected to air- CH_4 or air-CO gas flows (2500 ppm CH_4 or CO in air). The CO_2 gas resulting from catalytic oxidation was analyzed using Fourier Transform infrared (FTIR) spectroscopy of emitted gases. The intensities $I(t,T)$ of CO_2 vibrational bands was determined as a function of time (t) and temperature (T). The time dependence of these intensities was characterized by a first increase of $I(t,T)$ during an initiating period, then a stabilization for longer reaction times with a constant I_{max} value. The catalytic efficiencies of these

oxides were characterized from these intensities I_{max} of CO_2 vibrational bands. These I_{max} values increased with temperature. Figures 1 and 2 show the evolutions *versus* temperature of vibrational band intensities $I(t,T)$ of CO_2 gas formed from CO or CH_4 oxidations after a long oxidation period. In contradiction with theoretical predictions, a strong reactivity of lutetium oxide has been observed [3].

2.2. Mix system CeO_2 - Bi_2O_3 for catalytic applications

The system $[(1-x)\text{CeO}_2 - (x/2)\text{Bi}_2\text{O}_3]$ with $0 < x < 1$ has been elaborated at 600°C and a specific partial phase diagram has been observed with metastable Bi_2O_3 phases. The catalytic interactions between this system and air- CH_4 or air-CO flows are discussed. Low catalytic activity has been observed in the case of CH_4 interacting with the mix system, while strong activity is observed in the case of CO interacting with bismuth rich system. Figures 3 and 4 show the time dependent evolutions of vibrational band intensities $I(t,T)$ of CO_2 gas formed from CO or CH_4 oxidations after a long oxidation period.

2.3. Simulation of time dependent catalytic interactions

The observed intensities $I(t,T)_{\text{obs}}$ of CO_2 vibrational bands resulting from oxidations of CH_4 or CO have been interpreted through a unique time dependent model derived from the Avrami model, and describing the solid gas interaction mechanisms.

The modelling approach takes into account adsorption mechanism, degradation and regeneration of active catalytic sites subjected to oxygen and reducing gas interactions. The catalytic mechanism has been described

^a e-mail: gavarri.jr@univ-tln.fr

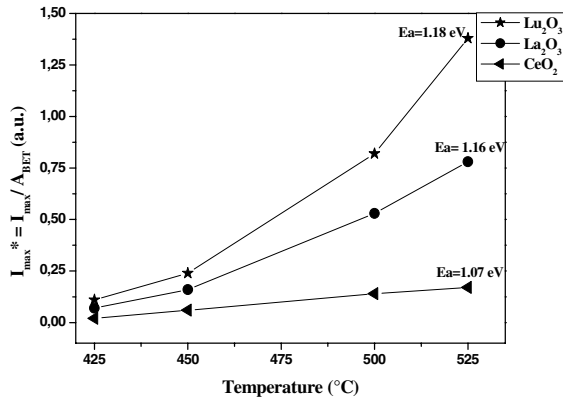


Figure 1. Evolution of maximum $I(t,T)$ values for CeO_2 , La_2O_3 and Lu_2O_3 reacting with air- CH_4 flows as a function of temperature.

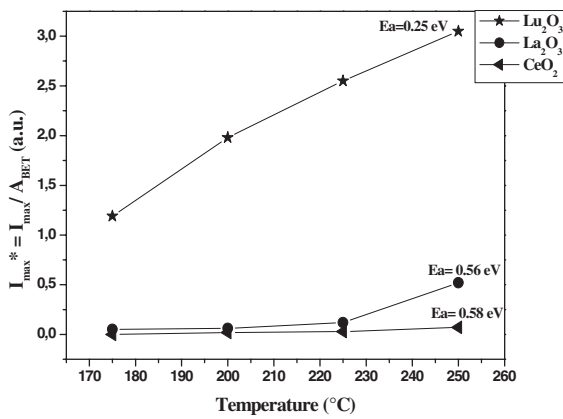


Figure 2. Evolution of maximum I^* values for CeO_2 , La_2O_3 and Lu_2O_3 reacting with air-CO flows as a function of temperature.

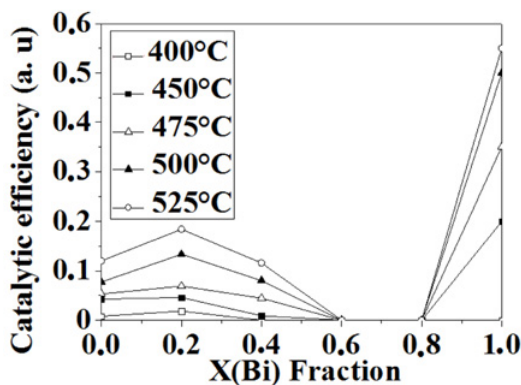


Figure 3. Conversion of CH_4 by $(1-x)CeO_2 - x/2Bi_2O_3$ samples as a function of Bi composition x , for fixed temperatures varying between 400 and 525 °C: normalized intensities I^* of CO_2 FTIR absorption bands, in arbitrary units.

in terms of three different functions derived from Avrami models:

- Adsorption of gas molecules: $A(t,T)$
- Reduction of active sites: $Red(t,T)$
- Oxidation of reduced sites from oxygen: $Ox(t,T)$.

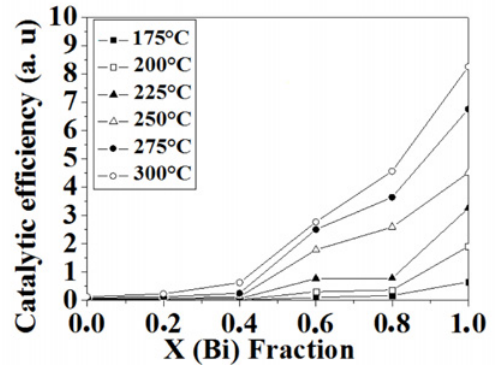


Figure 4. Conversion of CO by $(1-x)CeO_2 - x/2Bi_2O_3$ samples as a function of Bi composition x , for fixed temperatures varying between 175 and 300 °C: normalized intensities I^* of CO_2 FTIR absorption bands, in arbitrary units.

Table 1. Simulation parameters for solids interacting with air-CO gas flows or air- CH_4 gas flows at various temperatures.

Interacting with air-CO gas flows at 250 °C				
	La_2O_3	CeO_2	Lu_2O_3	Bi_2O_3
K_0	0.34	0.5	1.5	1.2
K_1	850	3	300	3
K_2	0.45	0.61	1.4	1.8
$S_1 = S_2$	60.5	6.7	305	500
Interacting with air- CH_4 gas flows at 525 °C				
K_0	0.5	0.2	0.58	0.4
K_1	100	15	20	10
K_2	0.6	0.68	0.4	0.5
$S_1 = S_2$	78.6	16.8	138.2	55

The amount of CO_2 resulting from oxidation of CH_4 or CO gases was then calculated from:

$$I(t, T) = A \cdot \{Red + Ox\}.$$

The $I(t,T)$ intensities were finally calculated from the expression :

$$I(t, T) = X_0 \cdot S \cdot [1 - \exp(-K_0 t)] \{ \exp(-K_1 t^2) + 1 - \exp(-K_2 t) \}.$$

The parameters X_0 , S are successively a scale factor and a surface activity factor. The K_0 , K_1 and K_2 parameters are successively kinetics constants of adsorption, site reduction and site oxidation.

The various parameters were determined to fit calculated curves $I(t,T)$ to experimental data. Table 1 gives a set of these parameters for one temperature.

Using these fitting parameters, calculated $I(t,T)_{calc}$ curves have been obtained in good agreement with the experimental data. The simulation approach allowed us to determine pertinent parameters for the two kinds of gas-solid interactions involving methane or carbon monoxide gases. The catalytic efficiencies of rare earth and bismuth oxides can be compared through these parameters.

Figures 5a,b and 6a,b show that the proposed model fits well the experimental data. It should be remarked that the experimental evolutions during the initiating period (short reaction times) can be well described by the proposed model.

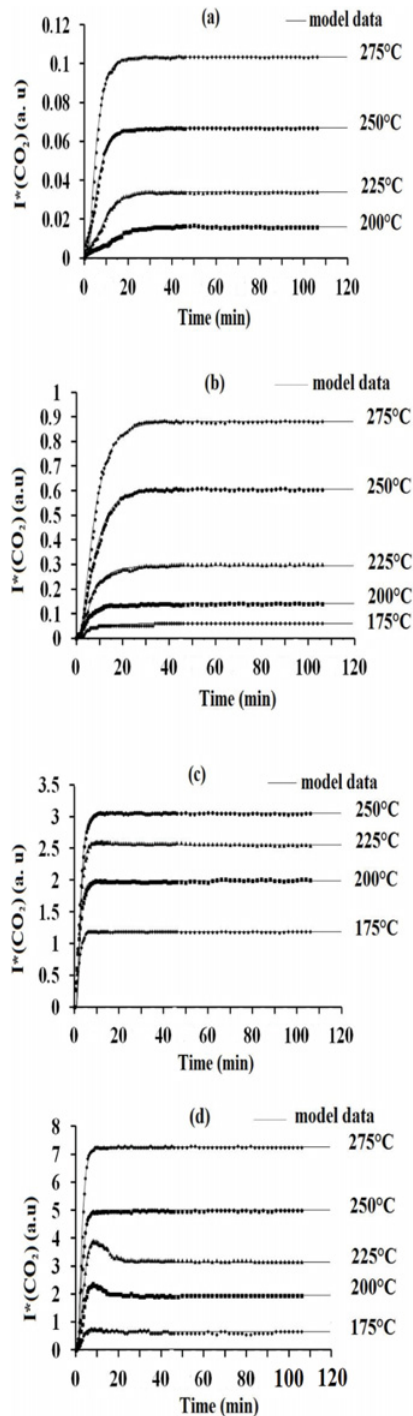


Figure 5. Simulation of CO oxidation efficiencies in the case of air-CO flows (2500 ppm CO) interacting with: (a) CeO_2 ; (b) La_2O_3 , as a function of time and for various temperatures; (c) Lu_2O_3 ; (d) Bi_2O_3 , as a function of time and for various temperatures.

3. HIGH TEMPERATURE ELECTROLYTIC APPLICATIONS

3.1. The electrical properties of CeO_2 - Bi_2O_3 system

The electrical properties of phases resulting from $[(1-x)\text{CeO}_2 - (x/2)\text{Bi}_2\text{O}_3]$ systems have been investigated using

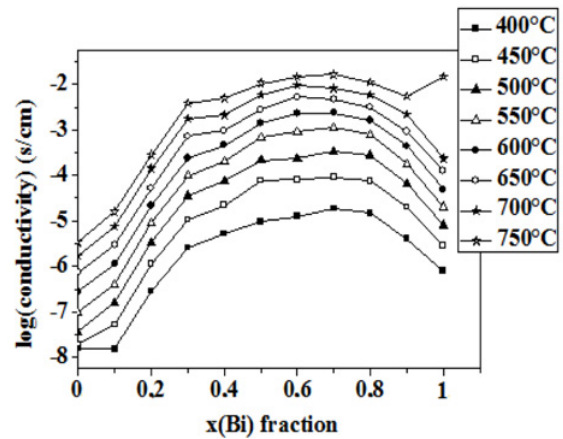


Figure 6. Evolution of sample conductivity for the system $(1-x)\text{CeO}_2 - (x/2)\text{Bi}_2\text{O}_3$ as a function of composition x and for various temperatures. The monoclinic transition is observed between 700 and 750 °C in the diagram ($x = 1$) with a large conductivity jump (in log scale).

impedance spectroscopy analyses in the temperature range 25 to 900 °C. The Nyquist representations of impedance data ($X = Z'$, $Y = -Z''$) have been discussed in terms of various models involving classical “constant phase elements” or Warburg impedances. In certain cases, an ionic conduction can be evidenced for bismuth rich phases. A maximum conduction has been evidenced in the case of the composite system with x close to 0.7. This behaviour might be directly related to the stabilization of the metastable β or β' Bi_2O_3 tetragonal phases coexisting with a substituted ceria phase and resulting from the specific elaboration process at 600 °C. This tetragonal phase is probably stabilized by the presence of small amounts of cerium ions in the Bi_2O_3 lattice. Figure 6 shows the variations of the logarithm of conductivity as a function of composition x in bismuth and of temperature.

4. DISCUSSION, CONCLUSION

4.1. Time dependent catalytic evolutions

The oxidation capacities of La_2O_3 , Lu_2O_3 , CeO_2 and Bi_2O_3 phases present three periods: a first initiating period, an intermediate period and a stabilization period (long reaction times). The Avrami model has been successfully used to describe these evolutions following an simple analytical function. Even abnormal variations in oxidation rates during the intermediate period can be described. One of the parameter (K_1) associated with a surface S_1 , can directly represent the activity of oxygen species initially adsorbed on grain surfaces and playing a role in the oxidation of gas traces in air flows.

4.2. Origin of oxidation efficiencies

In addition, we have observed that the two oxides Lu_2O_3 and Bi_2O_3 present high catalytic activities in the case of CO oxidation. The strong differences between the

catalytic activities of CeO_2 , La_2O_3 and Lu_2O_3 cannot be easily interpreted in terms of decreasing basicity or decreasing ionic radius. The nanostructured “acid” phase CeO_2 presents the lowest catalytic activity, while the Lu_2O_3 oxide behaves as a better catalyst. The role of 4f electrons in La ($4f^0$), Ce ($4f^1$), Lu ($4f^{14}$) was previously invoked to justify some catalytic evolution for rare earth oxides. However, in our experiments, there is no relation between the specific surfaces of catalysts and the observed catalytic efficiencies. In the case of Lu_2O_3 or Bi_2O_3 , their oxidation capabilities are necessarily bound to the nature of grain surfaces. It is the reason why, now, we are planning studies on the role of the specific nature of grain surfaces. As the solids are generally exposed to environmental atmospheres, it has been observed that environmental water and/or carbon dioxide could generate shells (thin layers) constituted of carbonate or oxy-carbonate based phases, enveloping grains. These shells might be at the origin of additional oxygen adsorption then exchange with CO and CH_4 [5,6].

4.3. Abnormal conductivity of Bi_2O_3

The high activity observed in the case of bismuth rich phases of CeO_2 - Bi_2O_3 system might be interpreted in terms of the presence of bismuth lone pairs (Bi^{3+}) and high oxygen mobility. In the case of presence of tetragonal metastable Bi_2O_3 phase, stabilized by cerium ions substituting for bismuth in the lattice, the high conductivity can be correlated to the large volume of structural “ Bi_2O_3 unit” and to weakly bound oxygen ions, these two factors being at the origin of the increasing ionic

mobility. At high temperature, the high ionic conduction due to the “ Bi_2O_3 open structure” should be responsible for the strong catalytic activity in CH_4 and CO oxidations.

We gratefully acknowledge the Provence–Alpes–Côte d’Azur Regional Council, the General Council of Var, and the agglomeration community of Toulon Provence Mediterranean for their helpful financial supports. This work was developed in the general framework of ARCUS CERES project (2008–2010).

References

- [1] B. Bakiz, F. Guinneton, M. Arab M, S. Villain, A. Benlhachemi, J-R. Gavarri, *Advances in Materials Science and Engineering*, ID 612130,4 pages, doi: 10.1155/2009/612130 (2009).
- [2] B. Bakiz, L. Bourja, A. Benlhachemi, Frédéric Guinneton, Madjid Arab, Jean-Raymond Gavarri, *Journal of Rare Earths* (2012).
- [3] L. Bourja, B. Bakiz, A. Benlhachemi, M. Ezahri, S. Villain, O. Crosnier, C. Favotto, J. R. Gavarri, *Journal Solid State Chemistry*, 184, 608–614 (2011).
- [4] L. Bourja, B. Bakiz, A. Benlhachemi, M. Ezahri, S. Villain, C. Favotto, J.-R. Gavarri *Advances in Materials Science and Engineering*, Volume 2012, ID 452383, 11 pages, doi:10.1155/2012/452383 (2012).
- [5] R. Alvero, A. Bernal, I. Carrizosa, J.A. Odriozola, J.M.Trillo. *J. Materials Science*, 22, pp. 1517–1520, 1987.
- [6] S. M. A. Rodulfo-Baechler, W. Pernia, I. Arayu, H. Figueroa, S. L. Gonzalez-Cortes. *Catalysis Letters*, 112, N° 3–4, 231–237, 2006.